

LETTER TO THE EDITOR

Herschel Observations of the W43 “mini-starburst” [★]

J. Bally¹, L. D. Anderson², C. Battersby¹, L. Calzoletti³, A. M. DiGiorgio⁴, F. Faustini³, A. Ginsburg¹, J. Z. Li⁵, Q. Nguyen-Luong⁶, S. Molinari⁴, F. Motte⁷, M. Pestalozzi⁸, R. Plume⁹, J. Rodon², P. Schilke¹⁰, W. Schlingman¹¹, N. Schneider-Bontemps¹², Y. Shirley¹¹, G. S. Stringfellow¹³, L. Testi¹⁴, A. Traficante¹⁵, M. Veneziani¹⁶, and A. Zavagno²

¹ Center for Astrophysics and Space Astronomy, Department of Astrophysical and Planetary Sciences, University of Colorado, UCB 389 Boulder CO 80309-0389, USA e-mail: john.bally@colorado.edu

² Laboratoire d’Astrophysique de Marseille (UMR 6110 CNRS & Université de Provence), 38 rue F. Joliot-Curie, 13388 Marseille Cedex 13, France

³ ASI Science Data Center, I-00044 Frascati (Rome), Italy

⁴ Istituto Fisica Spazio Interplanetario INAF, via Fosso del Cavaliere 100, 00133 Roma, Italy

⁵ National Astronomical Observatories, Chinese Academy of Sciences, Beijing 100012, China

⁶ Laboratoire AIM, CEA/IRFU CNRS/INSU Université Paris Diderot, CEA-Saclay, F-91191 Gif-sur-Yvette Cedex, France

⁷ Laboratoire AIM, CEA/DSM - CNRS Université Paris Diderot, DAPNIA/Service d’Astrophysique, Bt. 709, CEA-Saclay, 91191 Gif-sur-Yvette Cedex, France

⁸ Dept. of Physics, University of Gothenburg, 412 96, Göteborg, Sweden

⁹ Department of Physics and Astronomy, University of Calgary, 2500 University Drive NW, Calgary, AB T2N 1N4, Canada

¹⁰ I. Physikalisches Institut der Universität zu Köln, Zùlpicher Str. 77, 50937 Köln, Germany

¹¹ Steward Observatory, University of Arizona, 933 North Cherry Ave., Tucson, AZ 85721

¹² SAp-CEA/Saclay, 91191 Gif-sur-Yvette Cedex, France

¹³ Center for Astrophysics and Space Astronomy, University of Colorado, UCB 389 CASA, Boulder CO 80309-0389, USA

¹⁴ European Southern Observatory, Karl Schwarzschild str. 2, 85748 Garching, Germany

¹⁵ Dipartimento di Fisica, Università di Roma 2 “Tor Vergata”, Rome, Italy

¹⁶ Dipartimento di Fisica, Università di Roma 1 “La Sapienza”, Rome, Italy

Received 31 March 2010

ABSTRACT

Aims. To explore the infrared and radio properties of one of the closest Galactic starburst regions.

Methods. Images obtained with the *Herschel Space Observatory* at wavelengths of 70, 160, 250, 350, and 500 μm using the PACS and SPIRE arrays are analyzed and compared with radio continuum VLA data and 8 μm images from the *Spitzer Space Telescope*. The morphology of the far-infrared emission is combined with radial velocity measurements of millimeter and centimeter wavelength transitions to identify features likely to be associated with the W43 complex.

Results. The W43 star-forming complex is resolved into a dense cluster of protostars, infrared dark clouds, and ridges of warm dust heated by massive stars. The 4 brightest compact sources with $L > 1.5 \times 10^4 L_{\odot}$ embedded within the Z-shaped ridge of bright dust emission in W43 remain single at 4” (0.1 pc) resolution. These objects, likely to be massive protostars or compact clusters in early stages of evolution are embedded in clumps with masses of 10^3 to $10^4 M_{\odot}$, but contribute only 2% to the $3.6 \times 10^6 L_{\odot}$ far-IR luminosity of W43 measured in a 16 by 16 pc box. The total mass of gas derived from the far-IR dust emission inside this region is $\sim 10^6 M_{\odot}$. Cometary dust clouds, compact 6 cm radio sources, and warm dust mark the locations of older populations of massive stars. Energy release has created a cavity blowing-out below the Galactic plane. Compression of molecular gas in the plane by the older H II region near G30.684–0.260 and the bipolar structure of the resulting younger W43 H II region may have triggered the current mini-star burst.

Key words. Stars: protostars – Stars: massive – (ISM): HII regions – Infrared: ISM – ISM: W43

1. Introduction

The W43 “mini-starburst” region in the Molecular Ring near $l=30.8^{\circ}$ is one of the most luminous star forming complexes in the Galaxy (Motte, Schilke, & Lis 2003). Located at a distance of about 5.5 kpc at $V_{LSR} \approx 85$ to 107 km s^{-1} , W43 contains a giant H II region powered by a cluster of OB and Wolf-Rayet stars emitting a Lyman continuum luminosity of about 10^{51} ionizing photons per second (Smith, Biermann, & Mezger 1978; Lester et al. 1985; Blum, Damiani, & Conti 1999). The H II region is in contact with a 20 pc diameter giant molecular cloud (GMC) with

a mass of about $10^6 M_{\odot}$ (Liszt 1995) and a total IR luminosity of $\sim 3.5 \times 10^6 L_{\odot}$ (Lester 1985). Motte et al. (2003) identified about 50 clumps with masses ranging from 40 to 4,000 M_{\odot} in 350 and 1100 μm maps of the dust continuum.

W43 may be a “Rosetta Stone” for studies of super-star cluster formation using Hi-GAL data. Comparison of the Hi-GAL data with ground based radio data and space based *Spitzer* images show that on-going star formation is confined to a Z-shaped region abutting the W43 H II region.

2. Observations

Images of four square degrees centered at $l = 30^{\circ}$, $b = 0^{\circ}$ at wavelengths of 70, 160, 250, 350, and 500 μm were obtained

[★] *Herschel* is an ESA space observatory with science instruments provided by European-led Principal Investigator consortia and with important participation by NASA.

with the PACS (Griffin et al. 2010) and SPIRE (Poglitsch et al. 2010) instruments on the 3.5 m diameter telescope on the *Herschel Space Observatory* (Pilbratt et al. 2008) as part of the Science Demonstration Program for the Hi-GAL Galactic Plane Survey (Molinari et al. 2010). Each Hi-GAL image was “unsharp-masked” to suppress diffuse Galactic emission by convolving with a $\sigma = 70''$ gaussian to make a mask and subtracting this mask from the corresponding Hi-GAL image to enhance the visibility of small-scale structure ($< 200'' \sim 6$ pc).

3. Results

3.1. The W43 chimney: A young superbubble?

The *Herschel* images provide the first wide-field far-infrared views of the brightest portion of the Galactic plane near $l = 30^\circ$, allowing the investigation of the large-scale environment of the W43 mini-starburst complex (Figure 1). W43 lies at the top of the most prominent cavity in the four square-degree $l = 30^\circ$ *Herschel* field. The cavity consists of an S-shaped ‘hole’ in the dust emission bounded by a $6'$ radius curved ridge of dust extending from the left-side of W43 towards G30.772–0.209 and continuing to G30.684–0.260. Towards low-longitudes (right side of Figure 1) the cavity is bounded by a 0.25° -long vertical wall near $l = 30.5$. Most of the cavity interior is filled with faint free-free emission in the 20 cm MAGPIS VLA survey and the 5 GHz filled-aperture survey of Altenhoff et al. (1979). The cavity extends to at least Galactic latitude $b = -0.6$ where it becomes confused with the foreground H II region Sh2-67 at $V_{LSR} = 18$ km s $^{-1}$ ($d \sim 400$ pc; Fich, Treffers, & Dahl 1990) excited by BD-02 4752, a B0.5V star with visual magnitude 10.5.

The radial velocities of selected dust clumps were measured using emission from the 98 GHz CS 2–1 transition (Shirley et al. 2010) and with ^{13}CO 1–0 data from the FCRAO Galactic Ring Survey (Jackson et al. 2006). In Figures 1 and 3, CS radial velocities with 85 km s $^{-1} < V_{LSR} < 107$ km s $^{-1}$ are shown in yellow; radial velocities outside this range are shown in blue and cyan. Radial velocities based on ^{13}CO 1–0 are shown in with smaller yellow circles. The clouds located below W43, including the $6'$ radius ridge extending from the left side of W43 towards G30.772–0.209 and the wall near $l = 30.5$ are at $V_{LSR} \approx 99$ to 107 km s $^{-1}$. However, they appear to connect to the bright dust emission in W43. The larger radial velocities of these features compared to W43 may be due to acceleration by UV radiation and stellar winds. Although line-of-sight confusion by unrelated features is highly probable at $l = 30^\circ$, the preponderance of radial velocities similar to that of W43 make it likely that the Chimney is powered by massive young stars at a common distance of about 5.5 kpc. At this distance, the W43 Chimney is at least 70 pc long.

Infrared dark clouds (IRDCs) are seen in silhouette against background emission at wavelengths below $70 \mu\text{m}$ but are bright at wavelengths beyond $160 \mu\text{m}$. The cometary IRDC G30.772–0.209 and its bright rims (Figures 2 & 3) point towards G30.684–0.260 (IRAS 18456-0210). The 20 cm continuum and diffuse $24 \mu\text{m}$ *Spitzer* emission (not shown) indicate that massive stars are located just above G30.684–0.260. Figure 3 shows two concentrations of 6 cm mJy point-like radio sources in the MAGPIS survey (White et al. 2005; Helfand et al. 2006) that trace free-free emission from compact H II regions, ionized massive-star winds, or the brightest compact features in extended H II regions resolved by the VLA. The largest concentration is centered on W43 and a second group is located a few arcminutes below G30.684–0.260 around the UC H II re-

gion G30.667–0.332 embedded in a ^{13}CO cloud at $V_{LSR} = 89.4$ km s $^{-1}$. While the upper portion of the Chimney is clearly powered by W43, the southern portion appears to contain an older group of massive stars which produce the compact 6 cm sources, a diffuse H II region, and several cometary clouds.

3.2. The W43 starburst region

The W43 region is shown in detail in Figures 2 and 3. The 0.1° (~ 10 pc) long, Z-shaped W43 ridge of warm dust (red lines in Figures 1 and 3) is the brightest source of far-IR, sub-mm, and mm emission in the $l = 30^\circ$ field, and one of the brightest in the entire Galaxy (Smith, Biermann, & Mezger 1978). At $70 \mu\text{m}$, the Z-shaped ridge of bright dust emission contains a chain of about a dozen compact sources ($< 4''$ or 0.1 pc diameter) superimposed on the bright background of warm dust associated with the edges of the W43 H II region.

The Z-shaped ridge is situated at the ‘waist’ of a bipolar H II region that breaks-out towards both positive and negative Galactic latitudes. While the high surface-brightness lobe of W43 breaking out above the bar of the Z is confined to a 4 by 10 pc region, below the Z the lobe extends to the cometary clump G30.772–0.209 about $11'$ (~ 19 pc) from the W43 central cluster. Filamentary $70 \mu\text{m}$ dust emission closely follows the radio continuum emission at 20 cm in the MAGPIS survey and presumably traces warm dust in photon-dominated regions (PDR) located just outside ionization fronts illuminated by W43’s massive O and W-R stars. Ridges of colder dust seen absorption at $70 \mu\text{m}$ and below but in emission longward of $160 \mu\text{m}$ form arcs extending beyond the legs of the ‘Z’. The curved ridge which peels off the high-longitude end of the ‘Z’ is larger and forms a semi-circle of dust with a radius of about $6'$ (10 pc) and may be responsible for confining the eastern (low-latitude) lobe of the W43 H II region. This arc terminates in a prominent cometary clump, G30.772–0.209. A second chain of IRDCs extends from MM3 and wraps around the high-latitude side of the H II region, blocking its expansion in that direction.

G30.720–0.083 (= MM3 in Motte et al. 2003; 115 mJy at 6 cm) is the brightest compact H II region in the W43 complex. It is centered in a 1 pc radius IRDC seen in absorption at $70 \mu\text{m}$ and below and as a bright clump beyond $160 \mu\text{m}$. Prominent ionization fronts wrap around the side facing W43’s central cluster. G30.817–0.056 (= MM1) is located at the head of parsec-long cometary IRDC that faces the central part of the W43 H II region seen in silhouette at wavelengths less than $70 \mu\text{m}$. MM1 is not detected at 6 and 20 cm and may thus be in an earlier state of evolution than MM3. It is likely a massive proto-star or cluster of proto-stars exhibiting OH, H $_2$ O, and CH $_3$ OH masers (see Motte et al. 2003). At $4''$ (0.1 pc) resolution at $70 \mu\text{m}$, this and the other luminous sub-mm sources remain single and unresolved, implying that they are either isolated massive protostars, or clusters smaller than 0.1 pc.

The spectra of the four brightest compact sources, MM1 through 4 (Motte et al. 2003; marked in Figure 2) peak in the SPIRE $160 \mu\text{m}$ filter (Table 1). These FIR sources contain massive stars or compact clusters smaller than 0.1 pc in radius. The contribution of mid-IR emission below $60 \mu\text{m}$, and radiation that has escaped into the colder extended envelope (such as the 1 pc radius envelope around MM3) may raise the total luminosity of each to nearly $10^5 L_\odot$.

The unresolved emission from the 4 brightest MM sources provide about 2% of the total far-IR luminosity. The several dozen compact sources (Motte et al. 2003 listed 51) in the Z-shaped ridge may contribute an additional $\sim 6\%$. These compact

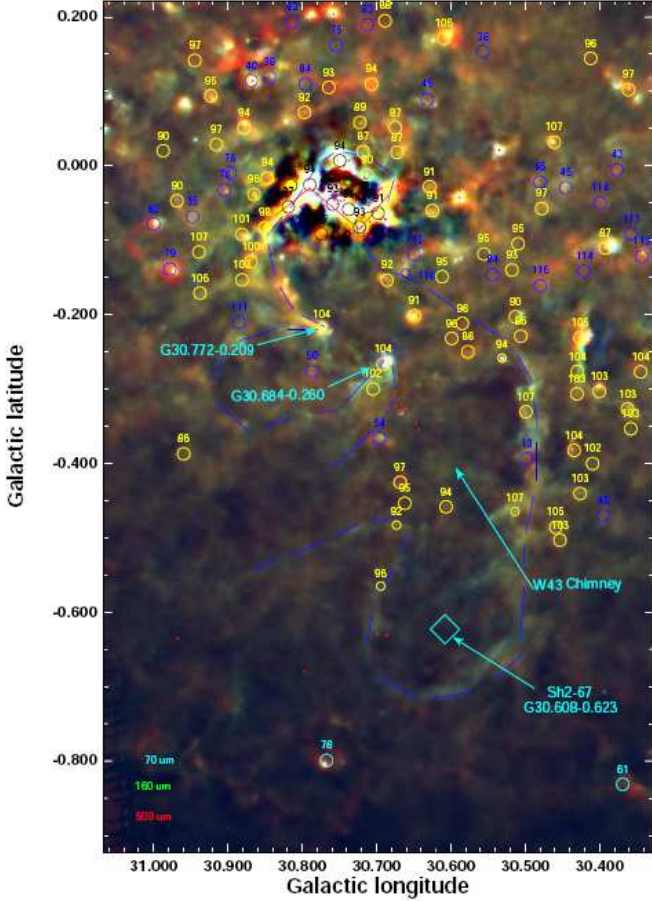


Fig. 1. A color composite image showing the W43 starburst region and the superbubble bursting towards low Galactic latitudes at 70 μm (blue), 160 μm (green), and 500 μm (red) using “unsharp-masked” images as described in the text. Small red circles or dots mark the locations of 6 cm point sources. Large yellow circles mark locations where the radial velocity has been measured using mm-wavelength tracers; yellow indicates radial velocities within the velocity range $85 < V_{LSR} < 107 \text{ km s}^{-1}$ measured using CS (Shirley et al. 2010, in prep.) or ^{13}CO . Blue and cyan circles indicate LSR velocities outside this range. Small yellow circles mark the locations of ^{13}CO clouds having similar radial velocities as W43. The numbers above each circle mark the LSR radial velocity in km s^{-1} . Several regions discussed in the text are marked in cyan. Warm dust at 70 μm outlines the walls of the “W43 Chimney” (shown in blue line segments). A 0.1° interval corresponds to a linear scale of 9.6 pc at the assumed 5.5 kpc distance to W43.

sources probably represent massive stars with $L > 10^4 L_\odot$ in various stages of formation. MM1 is probably the youngest since it is the most luminous in the far-IR, is associated with masers, but lacks free-free emission. MM3 is more evolved since it is associated with the brightest compact H II region at 6 cm, but still highly embedded within the Z-shaped ridge. Masses for the brightest compact sources are estimated using the 500 μm fluxes since the sources are most likely to be optically thin and on the Rayleigh-Jeans tail of the spectrum. We use the dust opacities from Ossenkopf & Henning (1994; OH94) for the bracketing cases of MRN grains without and with thin ice mantles evolved for 10^5 years at densities of 10^6 cm^{-3} . Dust temperatures listed in

Table 1. Properties of the Brightest Compact W43 Sources.

Source	S_{70}	S_{160}	S_{250}	S_{350}	S_{500}	$T(K)$	$L/[10^4 L_\odot]$	$M/[10^3 M_\odot]$
MM1	128	1943	1000	340	136	25	3.0	2.6 – 4.0
MM2	154	1400	700	246	164	23	1.5	3.5 – 5.3
MM3	277	1255	(400)	153	89	27	2.0	1.5 – 2.3
MM4	670	1148	205	131	53	28	2.0	0.9 – 1.3

- ^a Temperatures are determined from single grey body fits assuming an emissivity $\beta = 2$, and excluding the 70 μm data points.
- ^b Fluxes are in Jy. Luminosities only include flux from 60 μm to 600 μm and are based on fluxes within a Hi-GAL resolution element.
- ^c Masses estimated from $\lambda = 500 \mu\text{m}$ in a $37''$ beam, assuming OH94 opacities at $t = 10^5$ years, $n = 10^6 \text{ cm}^{-3}$ for thin ice mantles (first number) and un-evolved MRN dust with no mantles (second number).

Table 1 were determined using grey body fits to the SEDs. The best-fit Robitaille (2006) models are consistent with the envelope masses in Table 1, imply stellar masses around 10 to 23 M_\odot accreting at rates of around $10^{-3} M_\odot \text{ yr}^{-1}$. The beam-averaged envelope column densities range from $N(\text{H}_2) \sim 2 \times 10^{22} \text{ cm}^{-2}$ (MM4) to $\sim 1.6 \times 10^{22} \text{ cm}^{-2}$ (MM1).

The Hi-GAL data provides the best estimate of the total luminosity of the W43 complex which peaks around 160 μm , implying a typical dust temperature of around 20 K. Summing the fluxes in a $600''$ by $600''$ (16 pc) box centered on W43 yields a total far-IR luminosity of $L_{tot} = 3.6 \times 10^6 L_\odot$, within 10% of previous estimates (Lester et al. 1985). This is a lower limit since some radiation may escape to larger distances than the measurement box. Presumably, most of this luminosity is produced by the central WR+O cluster the massive stars traced by the 6 cm point sources and is reprocessed into the far-IR by the surrounding dust. Summing the total flux at 500 μm in this box, subtracting the background by averaging the surrounding annulus, assuming a grain temperature of 20 K, and a gas:dust ratio of 100 implies a total mass of $0.87 - 1.3 \times 10^6 M_\odot$ ($3.7 \times 10^6 M_\odot$ for un-evolved MRN grains).

WR stars are post-main sequence states of the most massive stars ($M > 60 M_\odot$) that have main-sequence lives of about 4 to 6 Myr. Thus, the age of the WR+O cluster in W43 is probably in this range. If massive stars have been forming at a constant rate over a 5 Myr period, the ratio of the luminosity of the 4 brightest objects, MM1 through 4, divided by the total luminosity of the region implies that the duration of the embedded massive protostar stage for such objects is $t_{proto} \sim L_{proto}/L_{tot} < 10^5$ years.

4. Discussion

There are at least two locations in the ‘W43 Chimney’ containing OB stars or associations; W43 and G30.684–0.260. Fich et al. (1990) have shown that G30.608–0.623 is likely to be associated with the foreground H II region Sh2-67. However, many molecular clouds associated with the dust rim surrounding this region have velocities similar to W43. Thus, these clouds are likely to be associated with the W43 chimney. Based on the dim 20 cm continuum, the large sizes of cometary clouds facing G30.684–0.260, and their location up to 20 pc away, the massive stars in this region (marked in part by the lower cluster of compact 6 cm sources in Figs. 1 and 3) must be older than W43.

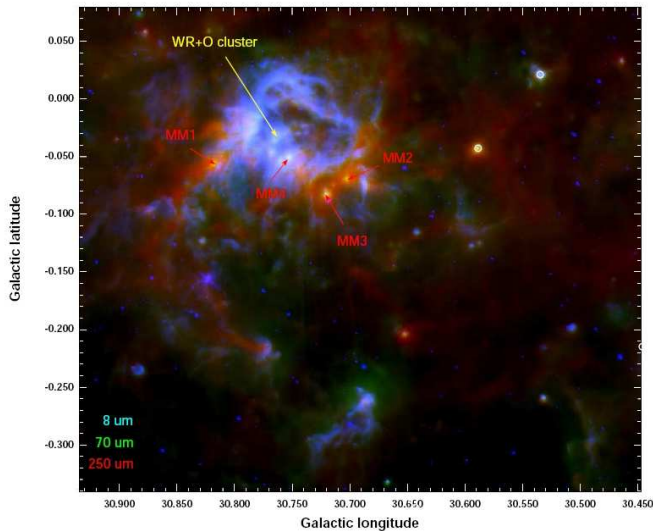


Fig. 2. A color composite image showing the W43 starburst region in the *Spitzer* 8 μm (blue), and Hi-Gal 70 μm (green) and 250 μm (red).

Ionization fronts up to 40 pc away along the $l = 30.5$ wall appear to be illuminated from this direction (Figure 1). Assuming a typical propagation speed of 5 km s⁻¹ for a typical D-type I-front moving through the ISM, the age of this cluster is likely to be 5 to 10 Myrs. We hypothesize that as the expanding H II region powered by this group impacted denser gas toward the Galactic plane, it triggered the formation and gravitational collapse of the GMC that evolved into W43, giving birth to its oldest massive stars (the O and WR cluster). Subsequently UV radiation from the central O+WR cluster compressed the parent cloud towards both low- and high Galactic longitudes, triggering the formation of additional massive stars.

The bipolar morphology of the W43 H II region indicates that its evolution has been constrained by dense gas associated with the warm 70 μm to 500 μm dust emission located in the horizontal central bar of the Z-shaped ridge. As the H II region expanded above and below the ridge, its pressure would have compressed it, possibly triggering the current ‘mini-starburst’ traced by the dozens of cores in the Z-shaped ridge.

The ‘W43 Chimney’ may be similar to but much younger than the superbubble emerging from the Orion OB association (Bally 2008) or the one powered by the IC 1805 cluster in the W4 complex (Basu et al. 1999). The Lyman continuum radiation and total luminosity of the W43 complex implies that it contains the equivalent of about 50 O7 stars. When these stars explode, they may cause the Chimney to blow out of the Galaxy to drive a ‘galactic fountain’.

5. Conclusions

Hi-GAL provides the first high resolution far-infrared view of the Galactic ISM. W43 contains about a dozen embedded massive protostars with $L > 10^4 L_{\odot}$ which contribute about 5% to 8% of the total luminosity, $L_{\text{tot}} = 3.6 \times 10^6 L_{\odot}$ measured in a 16 pc diameter box. The youngest luminous ($> 2 \times 10^4 L_{\odot}$) object, MM1 is located at the head of a comet-shaped IRDC pointing away from the W43 central cluster. MM3 is older since it is associated with the brightest compact H II region in W43. Compression of the Z-shaped filament by the bipolar W43 H II

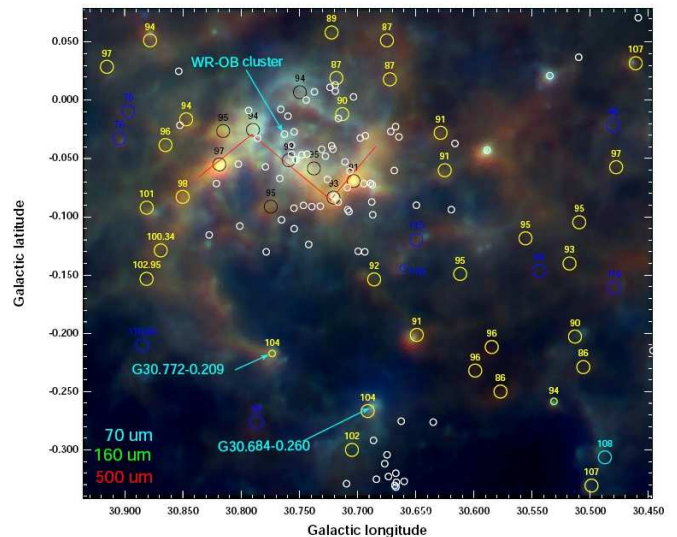


Fig. 3. A color temperature image showing the W43 starburst region at 70 μm (blue), 160 μm (green), and 500 μm (red). Small white circles mark the 6 cm point sources. Black circles mark the brightest Motte et al. (2003) MM sources with their radial velocities. As in Figure 1, yellow, blue, cyan, and red circles mark locations where radial velocities have been determined; the number above each circle give the LSR radial velocity.

region may have triggered the formation of dozens of luminous sources.

The ‘W43 Chimney’ is the most obvious giant cavity in the Hi-GAL fields and may represent a young 30 by 70 pc superbubble filled with diffuse 20 cm emission and rimmed by warm dust and molecular clouds having similar radial velocities as W43. Parsec-scale cometary clouds associated with G30.772-0.209 and G30.684-0.260 point to an older group of massive stars below W43 and associated with a cluster of compact 6 cm sources. Compression of clouds closer to the Galactic plane by this group may have triggered the initial burst of star formation in W43. W43 and this older group may be energizing the W43 Chimney.

Acknowledgements. The participation of J.B and G.S.S are supported in part by NASA through an award issued by JPL/Caltech via NASA Grant #1350780. We thank the referee for making excellent suggestions for improving the text.

References

- Altenhoff, W. J., Downes, D., Pauls, T., & Schraml, J. 1979, *A&AS*, 35, 23
- Bally, J. 2008, *Handbook of Star Forming Regions, Volume I*, 459
- Balser, D. S., Goss, W. M., & De Pree, C. G. 2001, *AJ*, 121, 371
- Basu, S., Johnstone, D., & Martin, P. G. 1999, *ApJ*, 516, 843
- Blum, R. D., Damiani, A., & Conti, P. S. 1999, *AJ*, 117, 1392
- Fich, M., Treffers, R. R., & Dahl, G. P. 1990, *AJ*, 99, 622
- Griffin, M. et al. 2010, *A&A*, (in press).
- Helfand, D.J., Becker, R.H., White, R.L., Fallon, A., & Tuttle, S. 2006, *AJ*, 131, 2525
- Jackson, J. M. et al. 2006, *ApJS*, 163, 145
- Lester, D. F., Dinerstein, H. L., Werner, M. W., Harvey, P. M., Evans, N. J., II, & Brown, R. L. 1985, *ApJ*, 296, 565
- Liszt, H. S. 1995, *AJ*, 109, 1205
- Molinari, S., & the Hi-GAL Team, 2010, arXiv, arXiv:1000.2106
- Motte, F., Schilke, P., & Lis, D. C. 2003, *ApJ*, 582, 277
- Ossenkopf, V. & Henning, T. 1994, *A&A*, 291, 943
- Pilbratt, G. L. et al. 2008, *SPIE*, 7010, 1
- Poglitsch, A. et al. 2010, *A&A*, (in press).
- Robitaille, T. P., Whitney, B. A., Indebetouw, R., Wood, K., & Denzmore, P. 2006, *ApJS*, 167, 256

Smith, L. F., Biermann, P., & Mezger, P. G. 1978, A&A, 66, 65
White, R.L., Becker, R.H., and Helfand, D.J. 2005, AJ 130, 586